



Dense nanocolumnar structure induced anti-corrosion CrB₂ coating with (0 0 1) preferred orientation deposited by DC magnetron sputtering

Jiahao Weng^{a,b}, Xiao Zuo^b, Linlin Liu^b, Zhenyu Wang^b, Peiling Ke^{b,c}, Xicheng Wei^a, Aiyang Wang^{b,c,*}

^a School of Materials Science and Engineering, Shanghai University, Shanghai 200444, China

^b Key Laboratory of Marine Materials and Related Technologies, Zhejiang Key Laboratory of Marine Materials and Protective Technologies, Ningbo Institute of Materials Technology and Engineering, Chinese Academy of Sciences, Ningbo 315201, China

^c Center of Materials Science and Optoelectronics Engineering, University of Chinese Academy of Sciences, Beijing 100049, China

ARTICLE INFO

Article history:

Received 5 November 2018

Received in revised form 14 December 2018

Accepted 2 January 2019

Available online 5 January 2019

Keywords:

CrB₂ coating

DCMS

Corrosion

Microstructure

(0 0 1) orientation

ABSTRACT

Superhard CrB₂ coatings with hardness around 45.7 ± 1.6 GPa were deposited on cemented carbide substrates via a direct current magnetron sputtering at the deposition temperature of 300 °C. The composition, microstructure and corrosion resistance of the deposited coatings were investigated. The results revealed that the deposited CrB₂ coating had a preferred (0 0 1) orientation and dense nanocolumnar structure. The great improvement in corrosion resistance of CrB₂ coated substrate was obviously observed from potentiodynamic polarization and electrochemical impedance spectroscopy. The formation of Cr₂O₃ was supposed to be the key factor for the obvious passivation phenomenon. Consequently, the corrosion current density was reduced by 100-fold in combination with a higher polarization resistance compared with the pristine substrate.

© 2019 Elsevier B.V. All rights reserved.

1. Introduction

With the development of marine economy and technology, marine equipment especially the moving components and parts are facing urgent corrosion problems. Hard coatings with good corrosion resistance have attracted more and more attention. Although traditional TiN/CrN coatings deposited by physical vapor deposition have excellent mechanical properties, they exhibit poor corrosion resistance due to the pinholes among the coarse columnar structure [1]. Other anti-corrosion coatings like Cr/GLC are lack of sufficient hardness, which limits their application under harsh abrasive conditions [2]. Therefore, it is of great importance to develop superhard coatings combining with outstanding corrosion resistance. Compared with the traditional carbide and nitride coatings, boride coatings have hexagonal alternately layered structure with stronger covalent bonds which benefit it high melting point, high hardness, good corrosion resistance and phase stability at the elevated temperature [3,4]. Till now, many research works have been concentrated on the hardness, wear and corrosion resistance of CrB₂ coatings prepared by pulsed DC and RF magnetron sputtering [5–7]. However, because of the low ionization degree,

it is rather tough to obtain the superhard CrB₂ coatings by traditional DC magnetron sputtering (DCMS). In our previous work, we have prepared superhard yet tough CrB₂ coating by DCMS at 300 °C [8]. In this work, we focused on the corrosion behavior of CrB₂ coating and discussed the corrosion mechanism of CrB₂ coating in terms of phase, composition and microstructure.

2. Experimental

CrB₂ coatings were synthesized on single-crystalline Si (1 0 0) wafers and cemented carbide (YG8, WC-8 wt% Co) substrates by DCMS with a thickness of around 3 μm. The sputtering current was controlled at 1.0 A. More detailed descriptions of deposition method and process can be found in Ref. [8]. The crystallographic structure of the coating deposited on YG8 was characterized by X-ray diffraction (XRD, Bruker D8 Advance diffractometer, Germany), with collecting angles ranging from 20° to 80° in conventional θ - θ configurations. Following with a focused ion beam (FIB, Auriga, Germany) process, the microstructure of the coating deposited on Si (1 0 0) was studied by transmission electron microscope (TEM, Tecnai F20, America). The mechanical properties including hardness and elastic modulus were tested using the continuous load-controlled nano-indentator (MTS NANO200). Electrochemical measurements were carried out on an electrochemical workstation

* Corresponding author.

E-mail address: aywang@nimte.ac.cn (A. Wang).

(Modulab, UK) in a 3.5 wt% NaCl solution. The electrochemical cell used a standard three-compartment cell which consisted of Ag/AgCl as a reference electrode, Pt as a counter electrode and sample as a working electrode. The potentiodynamic current-potential curves were recorded at a sweep rate of 1 mV/s. Electrochemical impedance spectroscopy (EIS) measurements were performed with a 10 mV amplitude signal under the open circuit potential, and the applied frequency was ranged from 100 kHz to 0.01 Hz. SEM (FEI Quanta FEG 250, America) and XPS (Axis ultradld, Japan) were applied to analyze the corrosion morphology and products after polarization tests.

3. Results and discussion

Fig. 1a shows the phase and microstructure of CrB₂ coating. Referring to the hexagonal CrB₂ PDF card (PDF34-0369), single (0 0 l) preferential orientation (including (0 0 1) and (0 0 2)) CrB₂ can be clearly discerned in Fig. 1a, where some weak WC peaks correspond to the YG8 substrate. (0 0 1) crystallographic plane is the closest-packed plane and has the lowest surface energy in CrB₂ compared with other orientations, so that it needs a long diffusion distance to be formed [9]. High deposition temperature causes an enhanced diffusion capacity of absorbed atoms which

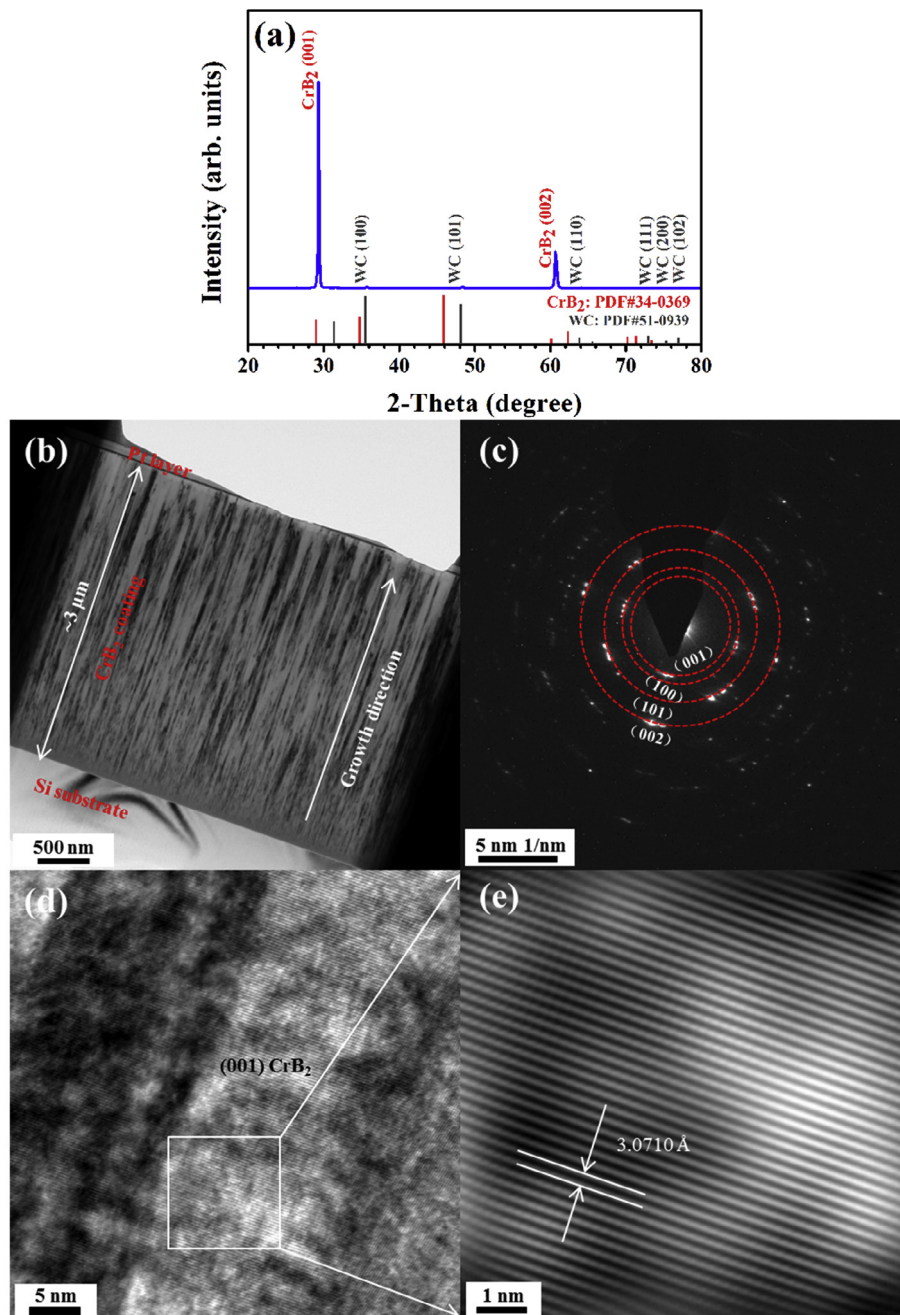


Fig. 1. Phase and microstructure of CrB₂ coating: (a) XRD pattern (b) low-magnification overview image (c) the corresponding SAED pattern (d) HRTEM image (e) the inverse fast Fourier transform image of (d).

gives rise to the formation of intense (001) texture. As shown in Fig. 1b and Fig. 1c, the thickness is about 3.0 μm and the coating exhibits uniform and dense nanocolumnar structure along the growth direction. (001), (002), (101) and (100) planes are identified from the SAED pattern. (101) and (100) peaks don't appear in XRD pattern because the extent of crystallization of these orientations is less than the minimum detection signal of XRD. Fig. 1d is a typical HRTEM image showing a clear crystalline area, and Fig. 1e is the inverse fast Fourier transform image. The lattice fringes spacing is 3.0710 \AA which corresponds to the (001) plane of CrB_2 .

The mechanical properties of CrB_2 coating are illustrated in Fig. 2a and b. As shown in Fig. 2a, the average hardness of CrB_2 coating is around 45.7 ± 1.6 GPa, which achieves the standard of

superhard coatings. Furthermore, we used the load-indentation depth curves to further study the elastic and plastic deformation of the coating in the indentation process. As depicted in Fig. 2b, both loading and unloading curves are smooth, no pop-in phenomenon is found in the curves, indicating a good compactness of the coating.

The corrosion resistance characteristics of CrB_2 coating and uncoated YG8 substrate are presented in the form of electrochemical impedance spectroscopy and potentiodynamic polarization curves. The EIS data is fitted using the equivalent circuit model (R(QR)). The larger radius of semicircular arc in Nyquist plots demonstrates the superior corrosion resistance of CrB_2 coating (Fig. 2c). The Bode plots in Fig. 2d also confirm the similar conclu-

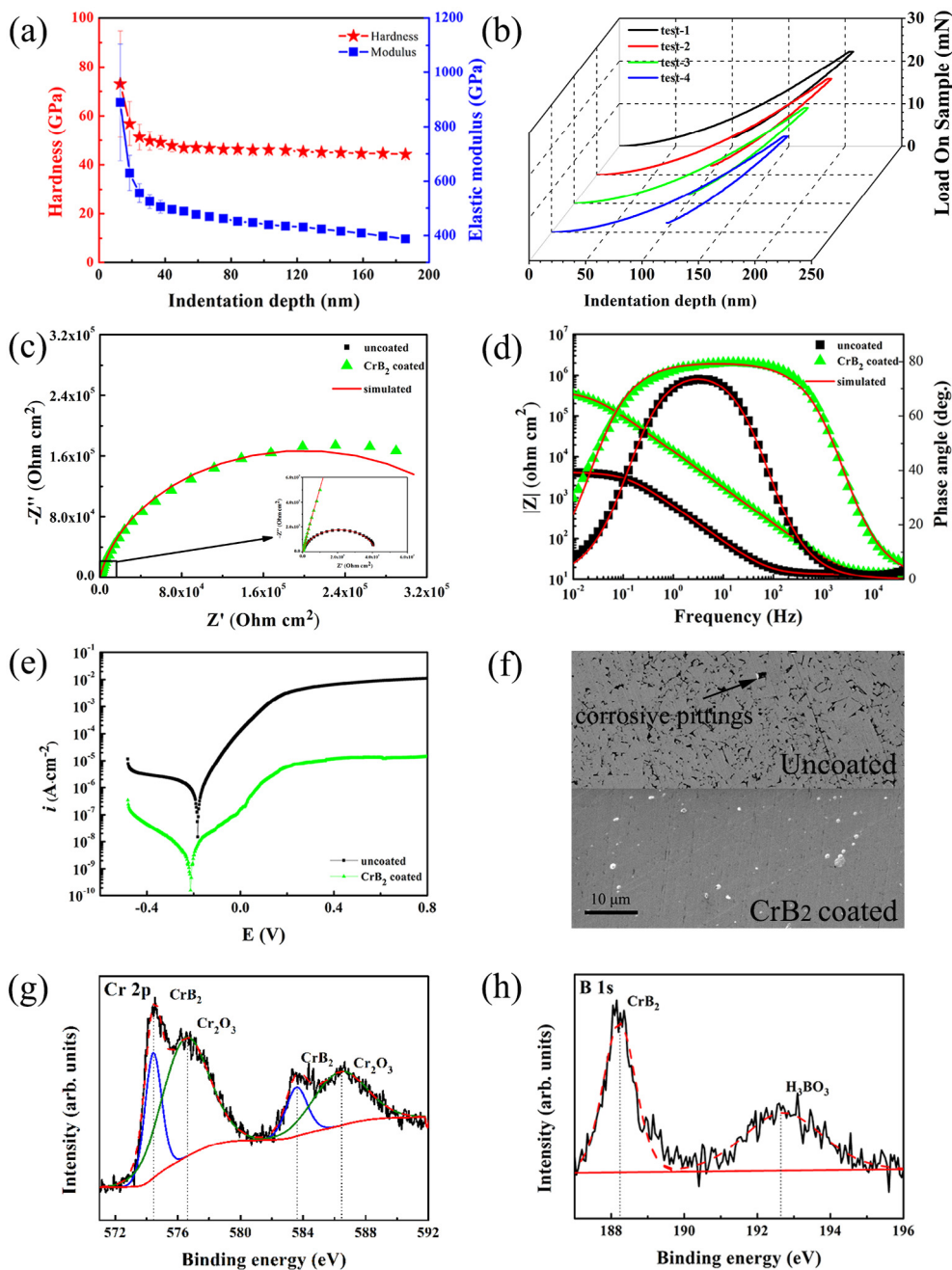
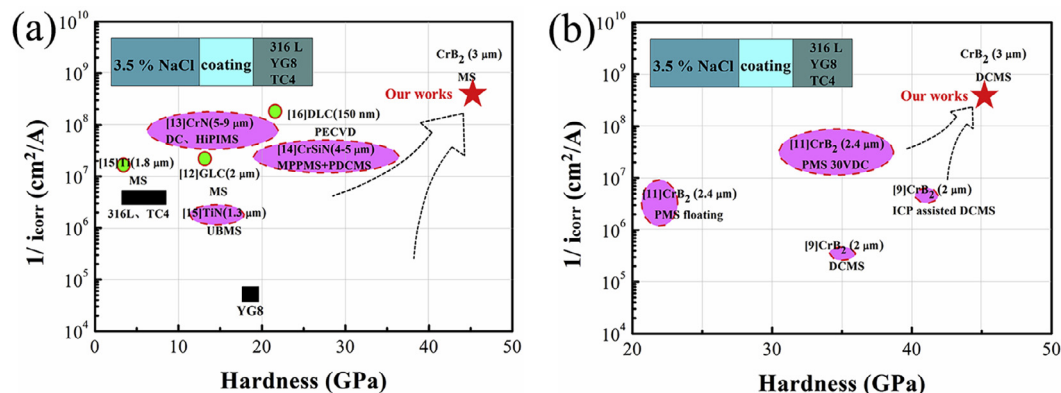


Fig. 2. Mechanical properties and corrosion resistance of CrB_2 coated and uncoated samples: (a) hardness and elastic modulus versus indentation depth curves (b) load-indentation depth curves (c) Nyquist plots (d) Bode plots (e) potentiodynamic polarization curves (f) surface morphology after polarization tests (g) Cr 2p spectrum of corroded coating (h) B 1s spectrum of corroded coating.

Table 1Corrosion potential (E_{corr}), corrosion current density (i_{corr}) and impedance parameters calculated according to the polarization curves and fitting circuit model.

Sample	E_{corr} (V)	i_{corr} ($\text{A}\cdot\text{cm}^{-2}$)	R_s ($\text{k}\Omega\cdot\text{cm}^{-2}$)	R_p ($\text{k}\Omega\cdot\text{cm}^{-2}$)
YG 8 substrate	-0.30	2.50×10^{-7}	13.43	4.19×10^3
CrB ₂ coating	-0.21	2.06×10^{-9}	12.98	3.99×10^5

**Fig. 3.** Improvement of hardness and corrosion resistance in this work compared with (a) other hard coatings (b) CrB₂ coatings.

sion. The larger $|Z|$ at low frequency as well as the phase angle near -90° in a wider frequency region indicate the excellent protective performance of CrB₂ coating to the substrate. The polarization curve of CrB₂ coating in Fig. 2e appears an obviously wide and stable passivation stage which is associated with a spontaneous passivation process formed in the corrosive medium. Fig. 2f is the surface morphology after polarization test. Numerous corrosion pits are found on the uncoated substrate which is owing to the dissolution of Co, while no obvious holes are found after the deposition of CrB₂ coating. The formation of Cr₂O₃ and H₃BO₃ obtained from XPS (Fig. 2g and h) could explain this phenomenon. This is due to the chemical reaction of CrB₂ in the corrosive medium [10].

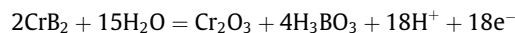


Table 1 summarizes the results of electrochemical experiments, where R_s is the solution resistance and R_p represents the polarization resistance. Nearly two orders of magnitude improvement in R_p is achieved by the addition of CrB₂ coatings. It can be seen apparently that the corrosion current density (i_{corr}) decreases about two orders of magnitude compared with the bare substrates. All these evidences have proved that the deposition of CrB₂ coating is able to enhance the anticorrosion capacity of YG8 substrate greatly. This outstanding performance can be explicated from three perspectives. Firstly, the dense nanocolumnar structure without micro-crack effectively reduces the diffusion of the aggressive medium. Furthermore, the growth of (0 0 1) textured CrB₂ coating endows the films with a better corrosion resistance [9,11]. Thirdly, the formation of Cr₂O₃ passive film also makes the coating less active. Compared with some recent work of other scholars [9,11–16], we have made a great progress in the fabrication of a superhard yet superior corrosion resistance coating (Fig. 3a and b).

4. Conclusion

In this work, CrB₂ coatings were deposited on cemented carbide (YG8) substrates through DCMS at 300 °C. The coating exhibited not only superhard mechanical properties but also outstanding corrosion resistance. These excellent performances were mainly caused by the preferred (0 0 1) orientation and compact

nanocolumnar microstructure brought by the high deposition temperature. The formation of Cr₂O₃ passive film also made the coating less active and explained the passivation phenomenon. This approach presented a promising candidate for the surface modification of cemented carbide to meet the requirements of marine engineering equipment.

Conflict of interest

None.

Acknowledgements

This work was financially supported by the National Natural Science Foundation of China (51522106, 51611130061), Zhejiang Key Research and Development Program (2017C01001), Ningbo Municipal Natural Science Foundation (2018A610175). We thank Prof. Magnus Odén for helpful discussion.

References

- [1] C. Liu, A. Leyland, Q. Bi, A. Matthews, Corrosion resistance of multi-layered plasma-assisted physical vapour deposition TiN and CrN coatings, *Surf. Coat. Technol.* 141 (2) (2001) 164–173.
- [2] L. Li, L.L. Liu, X. Li, P. Guo, P. Ke, A. Wang, Enhanced tribocorrosion performance of Cr/GLC multilayered films for marine protective application, *ACS Appl. Mater. Interfaces* 10 (2018) 13187–13198.
- [3] J. Menaka, S. Marka, M.G. Krishna, A.K. Ganguli, Multifunctional nanocrystalline chromium boride thin films, *Mater. Lett.* 73 (2012) 220–222.
- [4] U. Sen, S.S. Pazarlioglu, S. Sen, Niobium boride coating on AISI M2 steel by boro-niobizing treatment, *Mater. Lett.* 62 (16) (2008) 2444–2446.
- [5] M. Audronis, P.J. Kelly, R.D. Arnell, A. Leyland, A. Matthews, Deposition of multicomponent chromium boride based coatings by pulsed magnetron sputtering of powder targets, *Surf. Coat. Technol.* 200 (2005) 1616–1623.
- [6] M. Audronis, P.J. Kelly, R.D. Arnell, A.V. Valiulis, Pulsed magnetron sputtering of chromium boride films from loose powder targets, *Surf. Coat. Technol.* 200 (2006) 4166–4173.
- [7] K.L. Dahm, L.R. Jordan, J. Haase, P.A. Dearnley, Magnetron sputter deposition of chromium diboride coatings, *Surf. Coat. Technol.* 108–109 (1998) 413–418.
- [8] S. Zhang, Z. Wang, P. Guo, P. Ke, M. Odén, A. Wang, Temperature induced superhard CrB₂ coatings with preferred (001) orientation deposited by DC magnetron sputtering technique, *Surf. Coat. Technol.* 322 (2017) 134–140.
- [9] H.S. Choi, B. Park, J.J. Lee, CrB₂ coatings deposited by inductively coupled plasma assisted DC magnetron sputtering, *Surf. Coat. Technol.* 202 (4–7) (2007) 982–986.

- [10] L.R. Jordan, A.J. Betts, K.L. Dahm, P.A. Dearnley, G.A. Wright, Corrosion and passivation mechanism of chromium diboride coatings on stainless steel, *Corros. Sci.* 47 (5) (2005) 1085–1096.
- [11] M. Audronis, P.J. Kelly, R.D. Arnell, A. Leyland, A. Matthews, The structure and properties of chromium diboride coatings deposited by pulsed magnetron sputtering of powder targets, *Surf. Coat. Technol.* 200 (5–6) (2005) 1366–1371.
- [12] W.Q. Bai, Y.J. Xie, L.L. Li, X.L. Wang, C.D. Gu, J.P. Tu, Tribological and corrosion behaviors of Zr-doped graphite-like carbon nanostructured coatings on Ti6Al4V alloy, *Surf. Coat. Technol.* 320 (2017) 235–239.
- [13] C.R. Guimaraes, B.C.N.M. de Castilho, T.D.S. Nossa, P.R.T. Avila, S. Cucatti, F. Alvarez, J.L. Garcia, H.C. Pinto, On the effect of substrate oscillation on CrN coatings deposited by HiPIMS and dcMS, *Surf Coat Technol* 340 (2018) 112–120.
- [14] J. Lin, B. Wang, Y. Ou, W.D. Sproul, I. Dahan, J.J. Moore, Structure and properties of CrSiN nanocomposite coatings deposited by hybrid modulated pulsed power and pulsed dc magnetron sputtering, *Surf. Coat. Technol.* 216 (2013) 251–258.
- [15] K. Shukla, R. Rane, J. Alphonsa, P. Maity, S. Mukherjee, Structural, mechanical and corrosion resistance properties of Ti/TiN bilayers deposited by magnetron sputtering on AISI 316L, *Surf. Coat. Technol.* 324 (2017) 167–174.
- [16] S. Viswanathan, L. Mohan, P. Bera, V.P. Kumar, H.C. Barshilia, C. Anandan, Corrosion and wear behaviors of Cr-doped diamond-like carbon coatings, *J. Mater. Eng. Perform.* 26 (8) (2017) 3633–3647.